

A 2.5D Inversion of Airborne Electromagnetic data

Wing Wa Yu* and Eldad Haber, University of British Columbia

SUMMARY

In this work we implement an inversion algorithm for Airborne Electromagnetic data in the frequency domain by using 2.5D conductivity models. We discretize Maxwell's equations on a staggered 2D grid and solve the inverse problem by regularized minimization approach. We test the numerical accuracy of the forward solution and solve the optimization problem with a limited memory BFGS algorithm. The results of our 2D inversion are then compared to those from a well-established 1D implementation.

INTRODUCTION

In airborne electromagnetic (AEM) surveys, the spatial separation between survey lines is often big, and the survey is done parallel to the geology and therefore each magnetic field measurement does not extend noticeably into the adjacent lines. As a result, each flight line can effectively be inverted independently without too much of loss in resolution. This prompts to the use of 2D earth model to invert AEM datasets. Compared to 1D algorithms, 2D inversions have the advantage of enabling more accurate interpretation on conductive anomalies; and compared to 3D strategies, they require much less computing resources and are relatively trivial to parallelize for multi-core CPUs.

Over the past decades, numerous 2D EM algorithms have been designed using the well-known 2.5D formulation of Maxwell's equations (Stoyer and Greenfield (1976); Everett and Edwards (1992); Unsworth et al. (1993)). These algorithms, which have been applied to various airborne and controlled-source EM problems (e.g. Mitsuhata et al. (2002); Wilson et al. (2006); Abubakar et al. (2008); Key and Oval (2011)), are either based on finite element or finite difference approaches. But none used finite volume method, which we have preferred over FEM or FD, due to its simplicity in generating the matrix system, as well as its ability to handle high conductivity contrast.

In this work, we used the finite volume approach to implement an inversion algorithm for frequency AEM data. The algorithm was tested by inverting an AEM dataset from a Fugro RESOLVE survey that was carried out over the Red Dog mine site in Alaska. Our 2D results show strong agreement with models recovered by well-established 1D as well as 3D algorithm.

THEORY

Forward modeling

In our inversion scheme, each AEM survey line is inverted individually to recover the earth's conductivity. Underneath each line, we have assumed a 2D conductivity model that varies

only with the flight direction x and the depth z , and extends infinitely in the strike direction y : $\sigma = \sigma(x, z)$. These 2D slices are then as 2D cross-sections to build a quasi-3D earth model of the entire survey area.

By assuming 2D conductivity, the 3D Maxwell's equations can be reduced to a 2.5D form by applying the Fourier transform with respect to the strike direction y :

$$\tilde{F}(x, k_y, z) = \int_{-\infty}^{\infty} \vec{F}(x, y, z) e^{-ik_y y} dy. \quad (1)$$

Using the quasi-static approximation and a constant magnetic permeability, the 2.5D Maxwell's equations in the frequency domain when only electric sources are present are given by

$$\begin{aligned} \tilde{\nabla}_{k_y} \times \tilde{E} - i\omega\mu_0 \tilde{H} &= 0 \\ \tilde{\nabla}_{k_y} \times \tilde{H} - \sigma \tilde{E} &= \tilde{J}_s \end{aligned} \quad (2)$$

where \tilde{E} and \tilde{H} are Fourier transformed electric and magnetic fields, ω the angular frequency, \tilde{J}_s the current sources and $\tilde{\nabla}_{k_y} \times$ is the 2.5D curl operator which acts on a field quantity \tilde{F} like:

$$\tilde{\nabla}_{k_y} \times \tilde{F} = \begin{bmatrix} -ik_y \tilde{F}_z - \partial_z \tilde{F}_y \\ \partial_z \tilde{F}_x - \partial_x \tilde{F}_z \\ \partial_x \tilde{F}_y + ik_y \tilde{F}_x \end{bmatrix}. \quad (3)$$

Once a solution to (2) is obtained, it is converted back to 3D field using the discrete inverse Fourier transform:

$$\vec{F}(x, y, z) = \frac{1}{2\pi} \sum_{j=1}^N \tilde{F}(x, k_{y,j}, z) e^{ik_{y,j} y} g_j \quad (4)$$

where g_j is a weight for the wavenumber $k_{y,j}$. Since Eqn. (4) is an numerical approximation of the continuous inverse transform, for each given N the numerical error has to be minimized by optimizing for the wavenumbers and weights. This is done by using the optimization technique suggested in Xu et al. (2000) and Pidlisecky and Knight (2008) to find the optimum $k_{y,j}$'s and g_j 's for the magnetic field from a vertical magnetic dipole on the surface of a homogeneous half-space and then use the optimized values to compute responses due to other inhomogeneous half-spaces. In order to reduce computational cost, we have also picked the smallest N such that the error is still at a satisfactory level of less than 1% of the secondary field.

The 2.5D Maxwell's equations are solved by discretizing Eqn. (2) with finite volume method on a 2D staggered grid. Discretization of the field quantities and the conductivity on a unit cell are shown in Fig. 1. The fields are either discretized on the edges, at the nodes or in the cell-centers. The conductivity is discretized in the cell-centers and its value is assumed to be constant throughout the cell but jumps may occur at the boundaries. Our discretization is second order accurate for both the electric and magnetic fields and similar to 3D staggered grid discretizations, can deal with large conductivity contrast.

SEG extended abstract

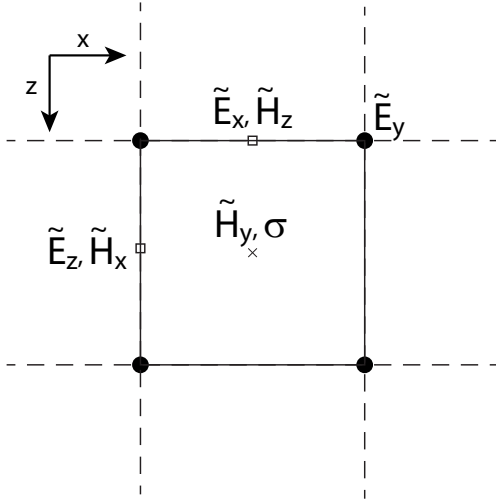


Figure 1: Discretization of 2.5D quantities on a staggered grid.

To compute the 3D fields, the following linear system resulted from discretizing Eqn. (2) has to be solved for each of the optimized values $k_{y,j}$:

$$\left(\mathbf{C}_{k_y}^T \mathbf{C}_{k_y} + i\omega\mu_0 \text{diag}(\mathbf{A}\sigma) \right) \tilde{\mathbf{E}}_{k_y} = -i\omega\mu_0 \tilde{\mathbf{J}}_s \quad (5)$$

$$\tilde{\mathbf{H}}_{k_y} = \frac{1}{i\omega\mu_0} \mathbf{C}_{k_y} \tilde{\mathbf{E}}_{k_y} \quad (6)$$

where \mathbf{C}_{k_y} is the matrix representation of the curl operator $\tilde{\nabla}_{k_y} \times$ and \mathbf{A} is a material averaging matrix that maps the cell-centered conductivity to the edges and the nodes. Each current source is modeled by a square loop of size L and the Fourier transform $\tilde{\mathbf{J}}_s$ for a loop centered at $(x_0, 0, h)$ is given by:

$$\tilde{\mathbf{J}}_s = J_0 \begin{bmatrix} iH_s(x-x_0) \sin\left(\frac{k_y L}{2}\right) \delta(z-h) \\ \left[\delta(x-x_0 - \frac{L}{2}) - \delta(x-x_0 + \frac{L}{2}) \right] \frac{\sin(k_y L/2)}{k_y} \delta(z-h) \\ 0 \end{bmatrix} \quad (7)$$

where h is the flight height, $\delta(x)$ is the delta function and $H_s(x)$ is the step function

$$H_s(x) = \begin{cases} 1 & |x| < L/2 \\ 0 & |x| > L/2 \end{cases} \quad (8)$$

Once $\tilde{\mathbf{H}}_{k_y}$ is computed for all $k_{y,j}$'s, the 3D magnetic response due to the conductivity σ is obtained using the conversion given by Eqn. (4).

Inversion framework

Given the observed magnetic field response, \mathbf{d}^{obs} , from a survey line, the goal of an EM inversion is to recover a conductivity model that minimizes the data misfit. Similar to other EM inverse problems, the log of the conductivity $m = \log(\sigma)$ is used and the data fitting is regularized by incorporating *a priori* information into the objective function. Here, we regularize with the most commonly used constraints in geophysical inversions; we require that the model is smooth and close to a

reference model. Therefore, we seek to minimize the following objective function:

$$\phi(m) = \frac{1}{2} \sum_i^{N_s} \left(\frac{d_i^{\text{pred}}(m) - d_i^{\text{obs}}}{\sigma_i^{\text{std}}} \right)^2 + \beta \left(\frac{\alpha_s}{2} \|m - m_{\text{ref}}\|_2^2 + \frac{\alpha_x}{2} \|\partial_x m\|_2^2 + \frac{\alpha_z}{2} \|\partial_z m\|_2^2 \right). \quad (9)$$

In Eqn. (9), β is the regularization parameter and d_i^{pred} is the computed magnetic field due to $\sigma = e^m$,

$$d_i^{\text{pred}} = \mathbf{P} \sum_j g_j \tilde{\mathbf{H}}_{k_{y,j}}(\sigma) \quad (10)$$

where \mathbf{P} is a measurement matrix. The first term of $\phi(m)$ is the squared sum of the data misfit, which is normalized by the noise standard deviation σ_i^{std} , over all N_s sources. The second term is the smallness regularization and the corresponding parameter, α_s , controls the length scale of the details in the inverted model. The smoothness in x and z -directions are controlled by the parameters α_x and α_z in the third and fourth terms and minimizing it has the effect of reducing sharp jumps in the recovered model.

In our work, the objective function is minimized using a quasi-Newton iterative method L-BFGS (Nocedal and Wright (1999)). In each iteration, a new model is computed using

$$m_{n+1} = m_n + \alpha \delta m_n \quad (11)$$

where α is a line search parameter and δm_n is the search direction given by the quasi-Newton approximate Hessian \mathbf{H} and the gradient:

$$\delta m_n = -\mathbf{H}^{-1} \nabla \phi(m_n) \quad (12)$$

In our solution, the Hessian is approximated by the L-BFGS method and the gradient is computed with

$$\nabla \phi(m) = \sum_i^{N_s} \left(\sum_j^N g_j \mathbf{J}_{k_{y,j}}^T \mathbf{P}^T \mathbf{Q}^{-1} (\mathbf{d}^{\text{pred}} - \mathbf{d}^{\text{obs}}) \right) \quad (13)$$

where $\mathbf{Q} = \text{diag}(\sigma^{\text{std}})$ and $\mathbf{J}_{k_y} = \frac{\partial \tilde{\mathbf{H}}_{k_y}}{\partial \mathbf{m}}$ is the sensitivity matrix. Note that the sensitivity does not have to be computed explicitly but instead only matrix vector products are needed (Haber et al. (2000)).

RESULTS

To evaluate the accuracies of our 2.5D EM formulation, numerical results of the forward solution were compared with known analytical solutions. To assess the validity of our inversion, models recovered with the 2D algorithm were compared to those obtained by well-established 1D inversion supplied by Fugro.

Numerical accuracy was tested by comparing the computed field response from a vertical dipole source on the surface of a homogeneous half-space to the analytical solution given in Spies and Frischknecht (1991). In Fig. 2, the responses at a distance of 10m from the source center are plotted for a half-space of $\sigma = 10^{-2} \text{ S/m}$ and for a range of frequencies typically

SEG extended abstract

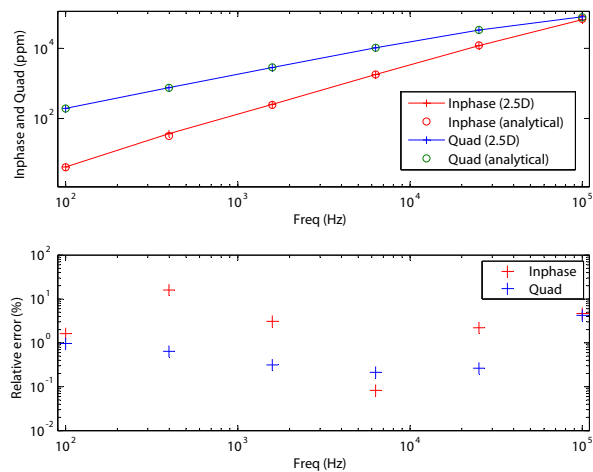


Figure 2: Comparison of numerical and analytical response. The responses at a receiver distance of 10m are plotted for a homogeneous half-space of $10^{-2} S/m$.

used in AEM surveys. We found that using only six optimized wavenumbers and a cell size of $10m \times 10m$ was enough to reduce the error to less than 5% of the theoretical value.

To check the effectiveness of our algorithm in inverting field data, we applied it on a RESOLVE dataset that was taken over the Red Dog mine in Alaska. In this survey, a total of 684 line kilometers were flown over the mine area at 50m spacing and in two orthogonal directions: 13° and 103° azimuth. The purpose of the survey was to detect conductivity contrasts in and around the tailing pond to search for any possible leakage of tailings from the waste area located to the east into the pond. Here, instead of running a full inversion on all the data points for each line, the data were resampled at 7% of the original sampling rate, which is equivalent to having a sounding every 40m. A mesh grid of size $8m \times 8m$ was used and the data were assigned a noise standard deviation of $\sigma^{std} = 10\% \times d^{obs} + 10^{-9} A/m$. By using an average value of β determined by the L-curve strategy and a convergence criteria of $\max(\delta\sigma_n) < 0.02 S/m$, convergence was usually reached within 50 iterations of L-BFGS(20). Each iteration took about 80sec on a cluster node outfitted with two 6-core Intel Xeon X5660 CPUs at 2.8GHz and 64 GB of memory.

Results of inversions performed on the two orthogonal survey lines highlighted in Fig. 3 are shown in Fig. 4. Despite high degree of variations in the data that are due to changes in the flight altitude, the predicted response showed a decent fit to a large portion of the observed data, as seen in Fig. 5. To further verify the reliability of our inversions, comparisons to models recovered with 1D algorithm were made. As demonstrated in Fig. 4, both the 1D and 2D models were able to resolve areas of high conductivity. These conductive regions were found to be at the pond and on top the waste dump area, and are related to the water in the pond and the conductive waste piled up on the dump site. We also observed that the sizes of the features seen in the 2D model were in general larger than those

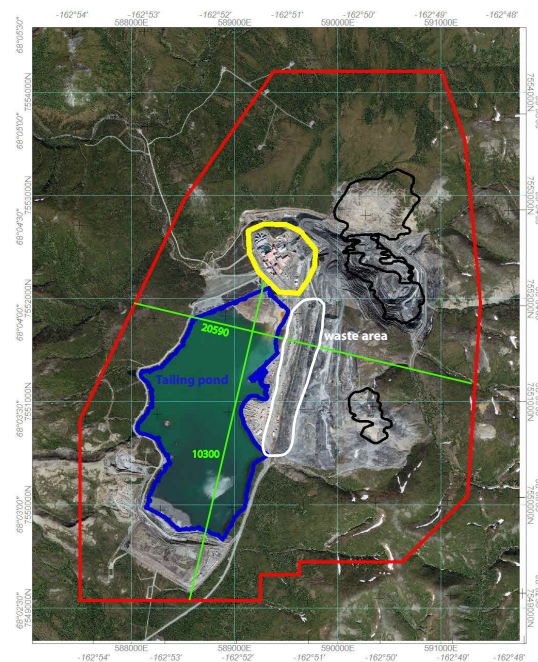


Figure 3: Map of the mine area. Red line: Outline of the survey area. Green lines: survey lines inverted.

in the 1D models. This is explained by our choice of a large smallness parameter α_s , which has the effect of eliminating small features in the recovered model. Despite the sizes of the recovered anomalies showed some discrepancy, their conductivity values found in the 2D results were in good agreement with the 1D results as well as their location and depth. These results provided us evidence that our 2D inversion algorithm is capable of resolving anomalous conductors and correctly identifying their conductivity.

CONCLUSION

The results shown here demonstrated that our 2.5D EM inversion algorithm can be successfully and reliably applied to frequency domain AEM data to locate and identify conductive anomalies. However, additional inversions with different regularization parameters should be performed to build more confidence about our model, and so that more decisive conclusions can be drawn about the anomalies. At last, it is worth to mention that there is work currently underway to implement a much faster algorithm which greatly reduces the number of grid cells by utilizing adaptively refined meshes (Haber et al. (2007)), as well as a 2D inversion code for time domain data.

ACKNOWLEDGMENTS

The authors wish to express their gratitude to Boris Lum and Joel Jansen of Teck Resources Ltd. for providing the RESOLVE dataset as well as useful information about the landscape of the mine area.

SEG extended abstract

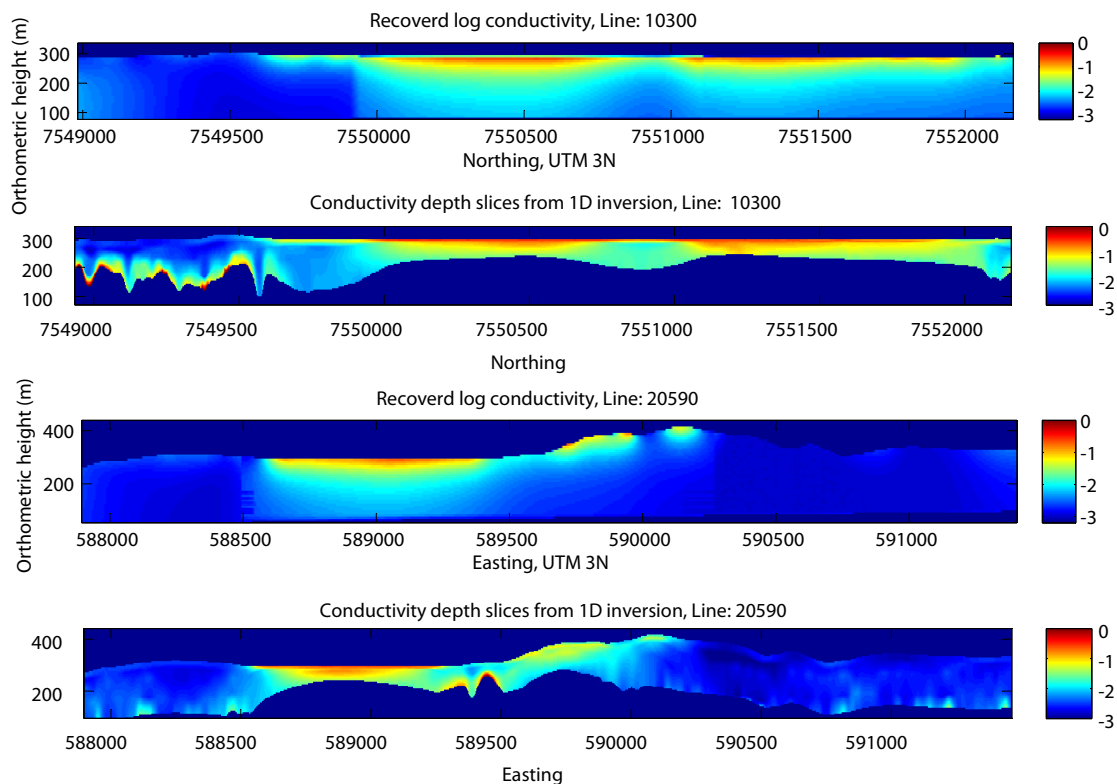


Figure 4: 1D and 2D inverted conductivity models for the two survey lines highlighted in Fig. 3.

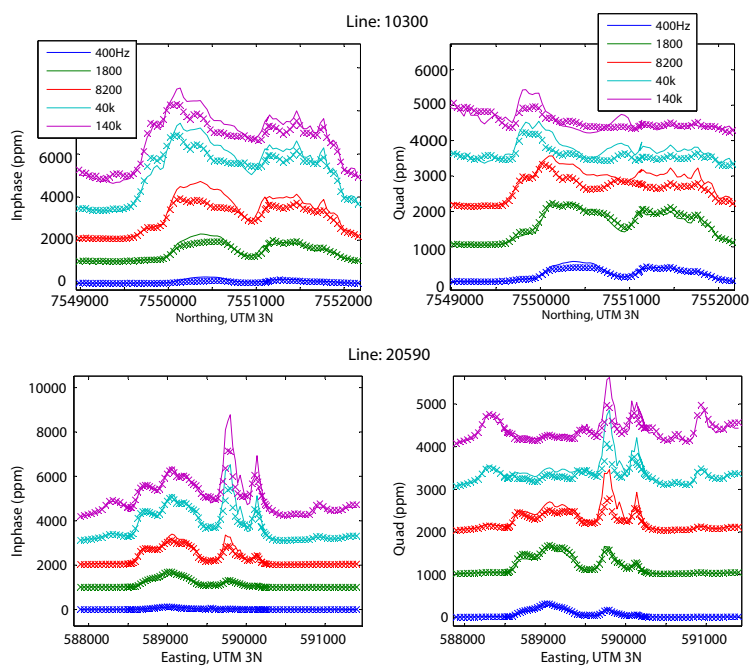


Figure 5: Data misfit for Line 10300 and 20590. The response curves have been offset by 1000ppm for clarity. Solid lines: predicted response. Crosses: observed data.

EDITED REFERENCES

Note: This reference list is a copy-edited version of the reference list submitted by the author. Reference lists for the 2012 SEG Technical Program Expanded Abstracts have been copy edited so that references provided with the online metadata for each paper will achieve a high degree of linking to cited sources that appear on the Web.

REFERENCES

- Abubakar, A., T. M. Habashy, V. L. Druskin, L. Knizhnerman, and D. Alumbaugh, 2008, 2.5D forward and inverse modeling for interpreting low-frequency electromagnetic measurements: *Geophysics*, **73**, no. 4, F165–F177, doi: 10.1190/?1.2937466.
- Everett, M., and R. Edwards, 1992, Transient marine electromagnetics: the 2.5-D forward problem: *Geophysical Journal International*, **113**, 545–561, doi: 10.1111/j.1365-246X.1993.tb04651.x.
- Haber, E., U. Ascher, and D. Oldenburg, 2000, On optimization techniques for solving nonlinear inverse problems: *Inverse Problems*, **16**, 1263–1280, doi: 10.1088/0266-5611/16/5/309.
- Haber, E., S. Heldmann, and U. Ascher, 2007, Adaptive finite volume methods for distributed non-smooth parameter identification: *Inverse Problems*, **23**, 1659–1676, doi: 10.1088/0266-5611/23/4/017.
- Key, K., and J. Owall, 2011, A parallel goal-oriented adaptive finite element method for 2.5-D electromagnetic modelling: *Geophysical Journal International*, **186**, 137–154, doi: 10.1111/j.1365-246X.2011.05025.x.
- Mitsuhata, Y., T. Uchida, and H. Amano, 2002, 2.5-D inversion of frequency-domain electromagnetic data generated by a grounded-wire source: *Geophysics*, **67**, no. 6, 1753–1768, doi: 10.1190/?1.1527076.
- Nocedal, J., and S. Wright, 1999, *Numerical optimization*: Springer.
- Pidlisecky, A., and R. Knight, 2008, FW2 5D: A MATLAB 2.5-D electrical resistivity modeling code: *Computers & Geosciences*, **34**, 1645, doi: 10.1016/j.cageo.2008.04.001.
- Spies, B. R., and F. C. Frischknecht, 1991, Electromagnetic sounding: *in* M. N. Nabighian, ed., *Electromagnetic methods in applied geophysics applications*: SEG.
- Stoyer, C., and R. J. Greenfield, 1976, Numerical solutions of the response of a two-dimensional earth to an oscillating magnetic dipole source: *Geophysics*, **41**, 519–530, doi: 10.1190/?1.1440630.
- Unsworth, M. J., B. J. Travis, and A. D. Chave, 1993, Electromagnetic induction by a finite electric dipole source over a 2-d earth: *Geophysics*, **58**, 198–214, doi: 10.1190/?1.1443406.
- Wilson, G. A., A. P. Raiche, and F. Sugeng, 2006, 2.5D inversion of airborne electromagnetic data: *Exploration Geophysics*, **37**, 363–371, doi: 10.1071/EG06363.
- Xu, S., B. Duan, and D. Zhang, 2000, Selection of the wavenumbers k using an optimization method for the inverse Fourier transform in 2.5D electrical modelling: *Geophysical Prospecting*, **48**, 789–796, doi: 10.1046/j.1365-2478.2000.00210.x.